Available online at www.sciencedirect.com
ScienceDirect
Nuclear Physics B (Proc. Suppl.) 196 (2009) 74–79
NUCLEAR PHYSICS B PROCEEDINGS SUPPLEMENTS
www.elsevier.com/locate/npbps

Telescope Array Experiment

Y.Tameda[a] for the Telescope Array Experiment*

[a] Tokyo Institute of Technology, 2-12-1, Ohokayama, Meguro-ku, Tokyo, 152-8550 Japan

The Telescope Array experiment (TA) is a hybrid detector situated in the USA consisting of a surface detector array and fluorescence detectors for observing extensive air showers produced by ultra high energy cosmic rays. The construction of the TA was finished and data taking with the hybrid observation started in March 2008.

1. Introduction

It has been predicted that the cosmic-ray energy spectrum has a limit above $\sim 10^{19.5}$ eV, the so called GZK cut off due to interaction with the cosmic microwave background[1],[2]. However the Akeno Giant Air Shower Array (AGASA) reported that 11 ultra high energy cosmic rays (UHECRs) with energy above 10^{20} eV were observed[3]. This result does not show the feature of the GZK cut off prediction. On the other hand, the energy spectra reported by the High Resolution Fly's Eye (HiRes)[4] and the Pierre Auger Observatory [5] are consistent with the GZK cut off. The systematic errors in determining the energy of these experiments are around 20% so the energy determination should be improved to conclude the contradiction.

The Telescope Array (TA) experiment is designed to study UHECR. The TA observatory is located in Millard County, Utah, USA(39.1°N, 112.9°W) at an average height 1400 m above sea level. TA is a hybrid detector consisting of a particle detector array of the AGASA type but much larger and fluorescence detectors (FD) which are also used for HiRes and Auger. The TA detector configuration is shown in Fig. 1. Three FD stations were constructed, one of them is transferred from HiRes-I and the others contain newly developed telescopes.

Hybrid measurements will be able to solve the problem of contradictions between the different detector types such as AGASA and HiRes. The energy scale of the SD can be calibrated by calorimetric measurement by FD. The geometrical reconstruction of SD can be cross-checked using FD stereo observations and that of the FD monocular will be improved using SD information.

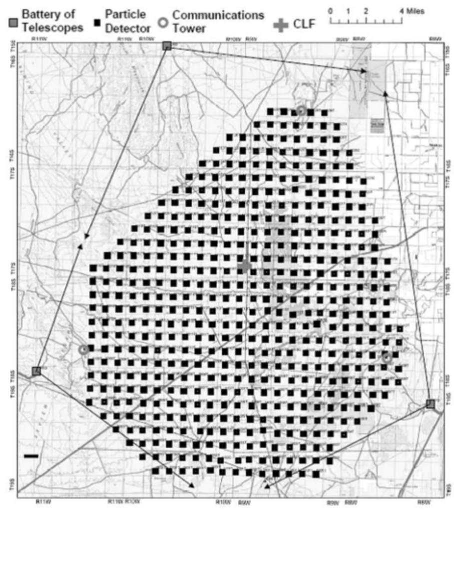

Figure 1. Detector configuration of the TA. (Black square: particle detector, Gray square: Fluorescence detector station, Circle: Communication tower, Cross on the center of the map: Central laser facility). Arrows represent the edge of field of view of FDs

The construction phase was finished by spring 2008, and the operation of all the FDs started

*E-mail: tame@cr.phys.titech.ac.jp

0920-5632/$ – see front matter © 2009 Published by Elsevier B.V.
doi:10.1016/j.nuclphysbps.2009.09.011

in Nov. 2007. The deployment of the surface detectors (SDs) was finished in March 2008 and the hybrid observation has started.

2. Telescope Array Experiment

2.1. Surface Detector

The TA SD array consists of 507 plastic scintillation counters arranged in a grid of 1.2 km spacing under the field of view of FDs. The detection area of TA SD is 678 km^2 and is 7 times larger than that of AGASA which is 100 km^2 with 111 counters. The trigger condition is for more than 3 neighboring counters each detecting 3 or more muons. The trigger efficiency reaches 100% for UHECRs with energy above $10^{18.7}$ eV with zenith angle less than 45°[7]. It's duty cycle is expected to be more than 95%.

Each detector consists of 2 layers of plastic scintillators 12 mm thick and 3 m^2 area separated by 1.0 mm stainless steel. 96 wavelength shifting fibers are installed in the grooves with 20 mm parallel intervals on the surface of each scintillator connected to photomultiplier tubes (PMTs, Electrontube 91245A). The gains of all SD PMTs are adjusted using cosmic ray muons remotely. The average number of photo electrons induced by a Minimum Ionization Particle is 24. The waveform signal through the low-pass filter with a cut-off frequency of 9.7 MHz is digitized by a 12 bit FADC whose sampling rate is 50 MHz. The system clock is synchronized with a Global Positioning System (GPS) and the accuracy of arrival timing is 20ns.

Figure 2 shows a deployed SD. Power is generated by the solar panel of 120W capacity and the electronics consumes $\sim$ 7W. A sealed lead-acid battery is also installed behind the panel. The SD array is divided into three areas to communicate for triggering and data acquisition by wireless LAN via an assigned communication tower in each. A boundary trigger can be achieved by communication between the towers and hybrid trigger supplied by FD and is now being planned.

2.2. Fluorescence Detector

There are three FD stations separated by 40 km around the SD array. HiRes-I was transfered to

Figure 2. One of the deployed surface detectors.

one of the northern stations at the Middle Drum (MD). There are 14 telescopes in this station each consisting of a spherical mirror of 2 m diameter and a PMT cluster at the focal plane. The effective mirror area is 3.75 m^2 and the curvature radius is 4.74 m. The field of view is 16.5° in azimuth and 16° in zenith. The HiRes-I sample and hold system is used for the electronics [6].

12 newly developed telescopes are installed in the other southern stations. The east station is at Black Rock Mesa (BRM) and the west station is at Long Ridge (LR). The spherical mirror optics with 3.3 m diameter, 6.8 m^2 effective area and 6067 mm curvature radius is combined by 18 hexagonal shape segment mirrors. The spot size at the focal plane is less than 30 mm. The field of view of each telescope is 15° in azimuth and 18° in elevation. The total field of view is 108° in azimuth and 3$\sim$33° in elevation.

A PMT camera is installed at the focal plane of the mirror. In each camera, 256 PMTs (HAMAMATSU R9508) are mounted in a 16 x 16 arrangement and covered with acrylic filter (KURARE paraglas). A UV transmitting filter (SCHOTT BG3) is attached in front of the PMT to reduce the night sky background. Each PMT has a 1.1°× 1.0° field of view. A negative high voltage is applied to each P and the gain is adjusted to 8×10^4. The PMT is DC-coupled in order to measure the night sky background di-

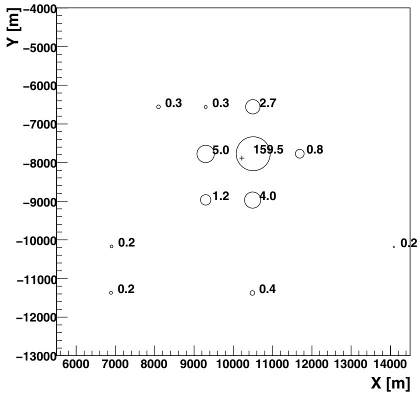

Figure 3. A typical SD event. Circles are hit detectors with radius proportional to the number of detected particles in logarithm.

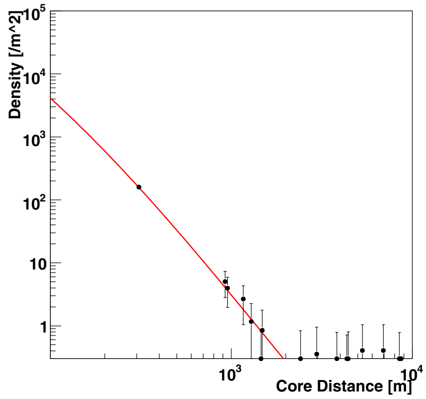

Figure 4. Preliminary analysis of lateral distribution of Fig. 3 event.

rectly.

The trigger electronics consists of the Signal Digitizer and Finder (SDF) module, the Track Finder (TF) module and the Central Trigger Distributor (CTD) module[8],[9] (Fig. 7). The whole triggering algorithm is programed by a Field Programmable Gate Array (FPGA). The PMT signal is amplified by a factor of 50 by the pre-amplifier and digitized by a 14 bit FADC mounted on the SDF with a sampling rate of 10 MHz. The SDF searches for a fluorescence signal by a sliding sum algorithm every 12.6 μs for a 25.6 μs time window. The first level trigger is generated when the moving average calculated by the SDF exceeds the threshold level which is adjustable by data acquisition software.

For each camera, the results of the first level trigger are accumulated to the TF to find air shower tracks. The criteria for the second level trigger is when 5 or more neighboring PMTs are triggered by the SDF. The results of the second level trigger in each FD station are sent to the CTD. If 3 or more PMTs are triggered on adjoining camera edges, the CTD also interpret this as an air shower track. Finally, the CTD sends a trigger pulse to all the electronics to acquire the waveform. The trigger rate of each FD station

Figure 5. Fluorescence detector station at Middle Drum and HiRes mirror units.

is ~3 Hz. The trigger efficiency for the primary energy above 10^{19}eV is shown in Fig. 8 which in stereo covers the whole SD area[10].

All the electronics are synchronized with a single clock (40 MHz) distributed by CTD. GPS is mounted on CTD to recored time stamps. If an aircraft flies into the field of view, the CTD also regards continuous triggers as a flash lamp to veto the trigger and the deadtime is also completely recorded.

2.3. Calibration and Atmospheric monitor

3 standard PMTs, the gain of which are calibrated absolutely by a standard light source be-

Figure 6. Fluorescence detector station at Black Rock Mesa.

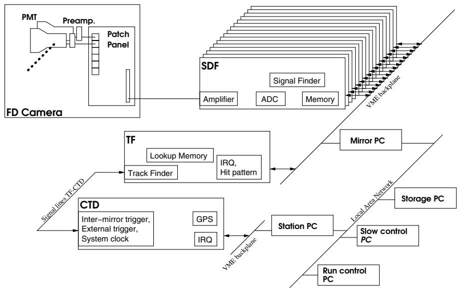

Figure 7. The block diagram of newly developed TA FD electronics.

fore installation[11], are mounted in each camera. The standard light source is the Rayleigh scattered light of a pulsed laser (Nd:YAG 335 nm) in nitrogen molecule gas. To adjust the gain of each standard PMT after installation, a YAP ($YAlO_3$:Ce) scintillator with ^{241}Am is attached in the UV transmitting filter. The gain of other PMTs are adjusted using a Xenon flash lamp as a uniform light source mounted at the center of mirror and compared with the standard PMTs. In observation terms, the gains of PMTs are monitored by YAP and Xe flash lamp. The gain uniformity of the PMT camera is measured once using the UV LED with XY-stage.

To estimate the amount of fluorescence light at the emitted point, the atmospheric profile should be monitored. The strategy of atmospheric monitoring used for TA are the LIDAR system and the Central Laser Facility (CLF). The LIDAR system consists of a Nd:YAG laser (355 nm) and a telescope with a PMT on a steerable base[12]. The back scattered light of the emitted laser pulse is accumulated by the telescope and detected by the PMT. Applying the slope method and Klett's method, atmospheric extinction coefficient and Vertical Aerosol Optical Depth (VAOD) are estimated.

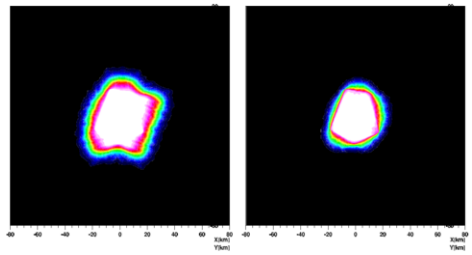

Figure 8. The trigger efficiency for the primary energy above 10^{19}eV with zenith angle less than 60°(left: monocular, right: stereo).

The CLF is located at the center of the FD stations[13]. A Nd:YAPG laser is used for the CLF and its shooting direction can be steered by the mirrors. The amount of scattered light induced by the emitted laser with 5mJ is equivalent to the fluorescence light generated by UHECRs with energy 10^{20} eV. To observe the CLF event by FD, atmospheric transmittance and VAOD can be estimated under the assumption of a one-dimensional aerosol distribution.

Moreover, a Linear Collider (LINAC) is developed as an end-to-end calibration system (Fig. 11). The TA-LINAC system can calibrate fluorescence yield and detector response such as mirror reflectivities, transparencies of filters, acrylic panel, QE × CE and the gains of PMTs at the same time. The TA-LINAC is locate 100 m from a BRM FD station so that atmospheric attenuation is negligible. The energy of the electron beam generated by the TA-LINAC is ∼40 MeV similar to a UHECR air shower with energy 10^{20} eV at a distance of 10 km. The assembly is almost fin-

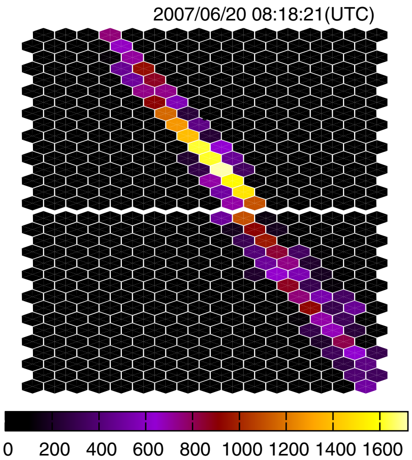

Figure 9. A typical air shower event.

ished and will be transfered in spring 2009[14].

3. Conclusion

By March 2008, the construction of TA, FD and SD was finished and data taking was started by hybrid observation. The CLF was installed by June, 2008 and started to shoot the test beam. The assembly and beam test of the TA-LINAC was almost finished and will be transfered to the site in spring 2009.

Acknowledgments

The Telescope Array collaboration wishes to acknowledge the support of the Japanese government through a Grant-in-Aid for Scientific Research (Kakenhi) on the Priority Area “The Origin of the Highest Energy Cosmic Rays”, the U.S. National Science Foundation (NSF) through awards PHY-0307098 and PHY-0601915 (University of Utah) and PHY-0305516 (Rutgers University), the Basic Research Program of the Korean Science and Engineering Foundation (KOSEF,Grant No. R01-2007-000-21088-0) and the Korea Research Foundation through KRF-2007-341-C00020. This work was supported by a 21st Century COE program at the Tokyo Institute of Technology “Nanometer-Scale Quantum Physics” by the Ministry of Education, Culture, Sports, Science and Technology.

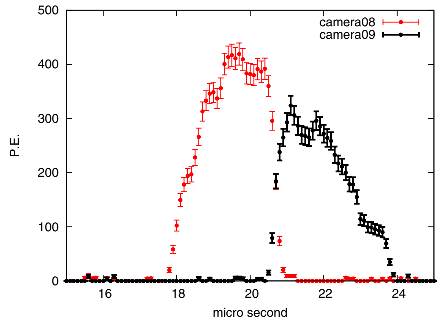

Figure 10. Time development of the air shower of Fig. 9 which are the FADC counts of triggered PMTs summed without background.

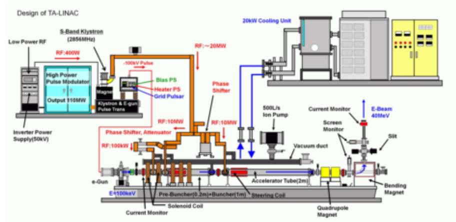

Figure 11. Schematic view of the TA-LINAC for the new calibration source for FD

REFERENCES

1. K. Greisen, Phys. Rev. Lett. 16 (1966) 748.
2. G.T. Zatsepin and V.A. Kuzmin, Sov. Phys. JETP Lett. 4 (1966) 78.
3. M. Takeda et al., Phys. Rev. Lett. 81 (1998) 1163.
4. R.U. Abbasi et al., Astropart. Phys. 23 (2005) 157.

5. J. Abraham et al., Phys. Rev. Lett. 101 (2008) 061101.
6. T. Abu-Zayyad et al., Nucl. Instr. Meth. A 450 (2000) 253.
7. N. Sakurai et al., Proc. of 30th ICRC, Merida 5 (2007) 1159.
8. A. Taketa et al., Proc. of 29th ICRC, Pune 8 (2005) 209.
9. Y. Tameda et al., Physica E 40/2 (2007) 430.
10. Y. Tsunesada et al., Proc. of 30th ICRC, Merida 4 (2007) 409.
11. H. Tokuno et al., Proc. of 30th ICRC, Merida 5 (2007) 1013.
12. M. Chikawa et al., Proc. of 30th ICRC, Merida 5 (2007) 1025.
13. S. Udo et al., Proc. of 30th ICRC, Merida 5 (2007) 1021.
14. T. Shibata et al., Nucl. Instr. Meth. A 257 (2008) 61.